Carbohydrate Research, 182 (1988) 1–17
Elsevier Science Publishers B.V., Amsterdam – Printed in The Netherlands

THE MOLECULAR STRUCTURE OF KAPPA-CARRAGEENAN AND COMPARISON WITH IOTA-CARRAGEENAN

RICK P. MILLANE, RENGASWAMI CHANDRASEKARAN, STRUTHER ARNOTT,
Whistler Center for Carbohydrate Research and Department of Biological Sciences, Purdue University, West Lafayette, Indiana 47907 (U.S.A.)

AND IAIN C. M. DEA
Leatherhead Food R.A., Randalls Road, Leatherhead, Surrey KT22 7RY (United Kingdom)

(Received April 29th, 1987; accepted for publication, October 15th, 1987)

ABSTRACT

The ordered conformation of kappa-carrageenan molecules in condensed but well-hydrated systems has been investigated by refining stereochemically plausible models to fit the continuous X-ray diffraction data obtained from oriented fibers. In the best model, the molecules are coaxial duplexes comprising right-handed, 3-fold helical chains of pitch 25.0 Å. As with iota-carrageenan, the chains are parallel but their juxtaposition in kappa-carrageenan is significantly different since they are offset from the half-staggered arrangement by a 28° rotation and a 1.0-Å translation. Alternative models (single helices, coaxial duplexes containing 6-fold chains, noncoaxial dimers, and mixtures of single and double helices) are quite incompatible with the diffraction data. Some antiparallel, coaxial duplex models approach the best model either in stereochemical plausibility or fit with the diffraction data, but none is as convincing overall as the best (parallel-stranded) model.

INTRODUCTION

Carrageenans are members of a family of gel-forming polysaccharides of the marine red algae *Rhodophyceae*. They are extracted commercially from seaweeds and used extensively in the food industry for gelling, thickening, bodying, and emulsion stabilization in both water-based and milk-based systems[1,2]. All carrageenans are linear polysaccharides of alternating (1→3)- and (1→4)-linked galactose units. Two principal gelling fractions of carrageenan, called kappa- and iota-carrageenan, are built up of alternating O-3 substituted β-D-galactopyranosyl and O-4 substituted 3,6-anhydro-α-D-galactopyranosyl residues. In both, most D-galactose units carry a half-ester sulfate group at O-4; the major difference between them is that most 3,6-anhydro-D-galactose units are sulfated at O-2 in iota- but not in kappa-carrageenan (Scheme 1). Between kappa- and iota-carrageenan, there is a continuum of intermediate compositions differing in degree of sulfation at O-2. The 3,6-anhydro-D-galactose content in kappa-type carrageenans varies, some

0008-6215/88/$ 03.50

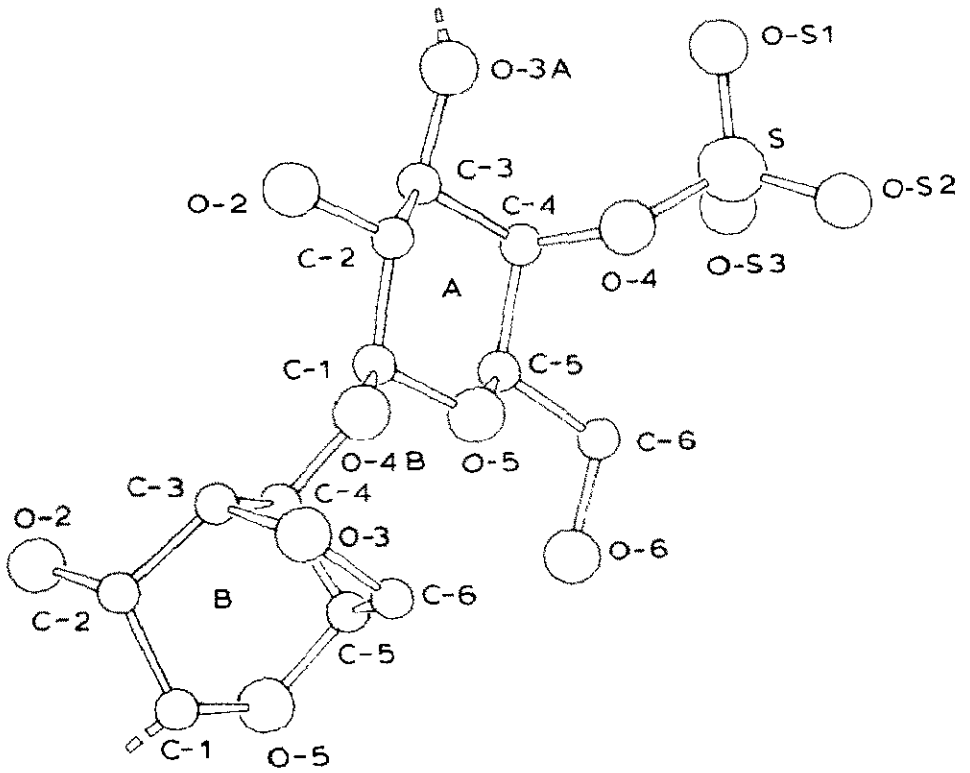

Scheme 1. Atom labeling scheme for a disaccharide of kappa-carrageenan: A is β-D-galactose 4-sulfate and B is 3,6-anhydro-α-D-galactose. For iota-carrageenan, B is sulfated at O-2.

residues being replaced by D-galactose 6-sulfate. In addition, a kappa-carrageenan variant exists in which only approximately 50% of the D-galactose residues are sulfated at O-4. This low sulfated gelling carrageenan is known as furcellaran[4].

Kappa- and iota-carrageenan, and furcellaran form thermally-reversible gels upon heating and cooling of aqueous solutions. The gelling mechanism is generally described as follows[4]. At temperatures above the melting point of the gel, the polymer chains exist in solution as random coils. On cooling, a three-dimensional polymer network in which double helices form juction zones between the polymer chains builds up. The formation of double-helical junction zones do not on their own, however, result in cohesive gel formation. Rather, crosslinking of up to 20 polymer chains to give noninteracting polymer domains occurs. Gel formation only results following the aggregation of the double-helical junction zones, which links the polymer domains into a complete three-dimensional gel structure. Thus, carrageenan systems which form nonaggregating double helices (*e.g.*, the Li^+ salt of iota-carrageenan) do not form gels[5].

Agarose is closely related structurally to the carrageenans. It differs only in having the (1→4)-linked 3,6-anhydro-α-D-galactopyranosyl residues replaced by the L-enantiomer, and being totally nonsulfated[6]. On decreasing the degree of sulfation from iota-carrageenan, through kappa-carrageenan and furcellaran, to agarose, the gels formed increase in rigidity, are less elastic and more brittle, and require lower concentrations of polysaccharide for their formation. For example, kappa-carrageenan forms gels at 1% concentration compared with 0.1% for agarose. For kappa-carrageenan, gelation shows cation selectivity, occurring in the presence of K^+, Rb^+, Cs^+, and NH_4^+, but not in the presence of Li^+ or Na^+. Kappa-carrageenan produces rigid, elastic gels with K^+ ions. In practice, some calcium

ions are always present resulting in a particularly high gel strength. Calcium ions alone give a stiff, brittle gel. As the percentage of O-2 sulfate groups increases, the potassium ion sensitivity decreases and there is a weakening of the gel properties. When 80% of the O-2 positions are sulfated, calcium ion sensitivity becomes predominant, and the properties become typical of those of iota-carrageenan[1]. An increased anhydrogalactose content increases both the potassium sensitivity and the gelling capacity. In aqueous systems, kappa-carrageenan exhibits synergistic cogelling properties with galactomannans, in particular locust bean gum, which are marked by an enhancement of the gel strength, a change from brittle to elastic gel rheology, and a reduction in syneresis. This property is not exhibited by iota-carrageenan. However, furcellaran exhibits enhanced cogelling properties with galactomannans, and agarose is even more effective[7]. It would appear that the mixed gelling interactions with galactomannans are favored by lower sulfate contents in carrageenans or agarose.

Earlier X-ray diffraction studies of oriented fibers of iota-carrageenan[8,9] have shown that it adopts a double helical structure in the condensed state. The double helix consists of two identical, parallel, right-handed, three-fold helices of pitch 26.6 Å which are displaced from each other along their common axis by exactly half the pitch. The double helix is stabilized by hydrogen bonds between OH-2 and OH-6 of the galactose residues in different chains.

Iota-carrageenan does not consist entirely of regular, alternating sequences of sugar residues; interruptions or "kinks" occur at various points in the chain which terminate double-helix formation. These "kinks" occur when the regular 3,6-anhydro-D-galactose residues are replaced by D-galactose, and can usually be removed by a Smith degradation procedure to create short blocks or segments, which retain the ability to form ordered structures but cannot gel[10]. Iota-carrageenan segments show a temperature-dependent sigmoidal increase in optical rotation, the sign and magnitude of which correspond closely to that predicted from the double-helix geometry in the solid state, when a semi-empirical calculation of optical activity based on the glycosidic angles of the polysaccharide backbone is used[11]. This optical rotation change has no thermal hysteresis and shows (at constant temperature and ionic strength) a concentration dependence which corresponds to a dimerisation process[12]. The order-to-disorder transition is also accompanied by an exact doubling of number average and weight average molecular weights[13]. Corroborative evidence for conformational ordering has also been obtained by high resolution ^{13}C- and ^{1}H-n.m.r. measurements. Sharp, well resolved spectra are obtained at 80°, when the polysaccharide exists as a disordered chain, which collapses on cooling to give the rigid ordered form[12]. Because of the "kinks" in the iota-carrageenan covalent structure, individual native polysaccharide chains combine with many partners on conformation ordering, resulting in a gelled structure. Iota-carrageenan gels show optical rotation changes analogous to those of the segments, and the midpoints for the transitions are close to the sol–gel temperatures. There is thus good evidence that the basic mechanism of cross-

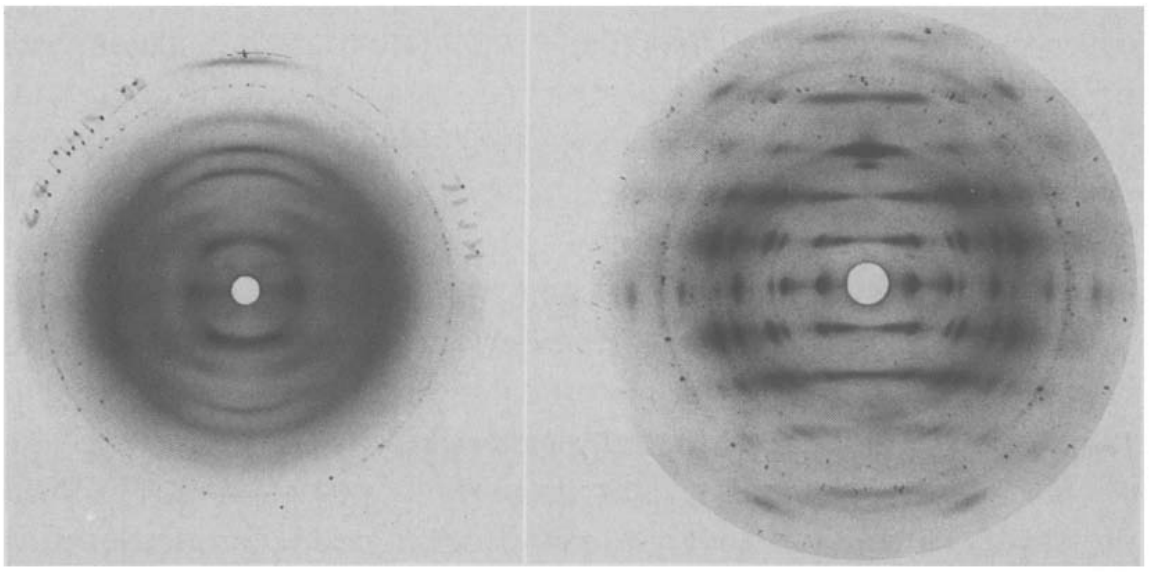

Fig. 1. Fiber diffraction patterns obtained from: (a) potassium kappa-carrageenan at 56% relative humidity (tilt of fiber to normal to incident X-ray beam is 10°); and (b) calcium iota-carrageenan at 75% relative humidity (fiber tilt 10°).

linking in the gel network is double-helix formation.

The case for kappa-carrageenan forming double helical-ordered conformations is less conclusive. Optical rotation measurements for segmented kappa-carrageenan show a cooperative concentration-dependent transition on heating and cooling, which provides good evidence that the ordered conformation exists in solution[14]. The transition shows hysteresis behavior, which can be correlated with aggregation of the ordered conformation. Similar optical rotation behavior is observed for native kappa-carrageenan on gel setting and melting. The hysteresis, however, is greater in the case of the gel, and this is interpreted as indicating that the degree of aggregation of the ordered conformation is higher. This random coil-to-helix transition has also been monitored by n.m.r. spectroscopy[15]. The dynamics of the salt (K^+)-induced disorder–order transition of native kappa-carrageenan have been studied by a polarimetric stopped-flow technique[16]. The results indicated that the formation of the ordered state is a second-order process and strongly supported the proposal that the aggregates of ordered chains in the junction zones of the gel comprise double-helical entities. The application[17–19] of the Manning polyelectrolyte theory indicated that the linear charge-density of the ordered structure is close to that expected for a dimeric species. Until this study, there was no specific evidence for double-helix formation, however. Indeed, the possibility that the important ordered conformation in kappa-carrageenan is a single-chain helix has been postulated[20,21] on the basis of optical rotation measurements in the presence of I^- ions. Moreover, the diffraction patterns from kappa-carrageenan fibers (*e.g.*, Fig. 1) exhibited intensities on layer lines with spacings of 25.0 Å. Analogous spacings are systematically absent from iota-carrageenan patterns because of the half-staggered, coaxial arrangement of parallel helices. It follows that the ordered conformation of kappa molecules is significantly different from that of iota molecules. Whether this is simply deviation from the half-staggered

arrangement or something more profound could not conveniently be investigated by diffraction analysis until recently, as kappa-carrageenan molecules in fibers can be uniaxially oriented but not further organized laterally into microcrystallites. The diffraction from such systems consists of layer lines of continuous intensity rather than the sharp arcs from crystalline systems. Only recent advances[22,23] in collecting and processing diffraction data of the former type made it possible to conduct detailed analyses of alternative models.

Obvious candidate models are coaxial duplexes with parallel but not half-staggered chains, or single-stranded molecules with conformations similar to one chain of an iota duplex. Coaxial duplexes with antiparallel chains would also preserve the 25.0-Å layer line spacings as would duplexes with parallel half-staggered six-fold chains of pitch 50.0 Å. A system with ordered single-strands, some of which might be involved in iota-like half-staggered duplexes, is plausible, and it is also conceivable that the molecules could be organized as duplexes but without the chain axes coinciding.

EXPERIMENTAL

Sample preparation. — The samples of kappa-carrageenan used (code REX 5104 obtained from Marine Colloids Inc., Rockland, Maine 04841, U.S.A.) were from *Chondrus crispus*. Kappa-carrageenan from *Chondrus crispus* normally is highly sulfated at O-2 of the 3,6-anhydro-D-galactose units (~25%). However, REX 5104 is a special fraction of *Chondrus crispus* kappa-carrageenan having a low (3%) degree of sulfation at O-2, and is therefore close to that of an ideal kappa-carrageenan. The sample was converted into the K salt by ion-exchange chromatography on Amberlite IR-120 resin, and oriented fibres were prepared conventionally[24] at room temperature and 56% relative humidity.

X-ray intensity data. — X-ray diffraction patterns were recorded with flat-film pinhole cameras using Ni filtered CuKα radiation. Spacings were calibrated by dusting the specimens with calcite (d = 3.035 Å). The optical densities on the diffraction pattern were digitized with an Optronics Photoscan P-1000 rotating drum microdensitometer. The center and orientation of the diffraction pattern, fiber tilt to the X-ray beam, and c-repeat were determined by use of standard methods[25]. A two-dimensional background function expanded as a Fourier–Bessel series was calculated from optical densities at positions between the layer-lines and then subtracted from the original diffraction pattern[22]. Because the layer-lines overlap with each other except at low resolution, samples of the intensity at 0.01 $Å^{-1}$ intervals along the individual layer-lines were determined by use of a profile-fitting procedure[23] based on the method of angular deconvolution[26]. This sample spacing is $\sim 1/3$ of the minimum necessary for a molecular diameter of 15 Å (ref. 23). The measurements were corrected for oblique intersection of the angular profile with the layer-lines, and for Lorentz and polarization effects. The basic angular intensity profile due to disorientation was estimated on layer-lines at

positions close to the center of the pattern, where there is no overlap. The maximum resolution (~4 Å) on each layer-line to which data were collected was determined by the reliability with which they could be separated.

Model building. — The conformation of the D-galactose ring was derived from the standard conformation[27] of β-D-glucopyranose with appropriate inversion of the configuration at C-4. The atom-labeling scheme used throughout is shown in Scheme 1. All hydrogen atoms were included. The geometry of the 3,6-anhydro-D-galactose unit was taken from the crystal structure of methyl 3,6-anhydro-α-D-galactopyranoside[28]. The two glycosidic bridge angles were set at 116.5°, the bond angles at the ester oxygen atoms at 116.0°, and all other bond angles in the sulfate group at 109.5°. The S–O ester bond lengths were set to 1.60 Å, and all other S–O bonds at 1.45 Å. The four conformation angles at the glycosidic oxygen bridges and the three defining the side-group orientations were initially set at the values determined for iota-carrageenan[9]. Molecular models of an isolated chain of designated pitch and chirality were generated by use of the linked-atom least-squares (LALS) technique[29,30].

X-ray refinement. — The LALS technique, modified to include continuous X-ray data, was used to refine each molecular model to achieve minimum steric compression and best fit with the X-ray data. Variable parameters were the four conformation angles at the glycosidic bridges, the two defining the sulfate group conformation, and the one defining the hydroxymethyl group orientation, and an X-ray scale factor. The variable parameters were adjusted so as to minimize (in a least-squares fashion) the Expression (*1*). Preferred conformational domains are

$$\Omega = \sum_{k=1}^{N_e} e_k \Delta\theta_k^2 + \sum_{m=1}^{N_c} \omega_m \Delta F_m^2 + \sum_{i=1}^{N_c} k_i \Delta d_i^2 + \sum_n \lambda_n G_n \qquad (1)$$

$$= \quad E \quad + \quad X \quad + \quad C \quad + \quad L$$

achieved by elasticating conformation angles (θ_k) to their respective expected values, and they constitute the first term E. The term X involves the differences (ΔF_m) between the observed X-ray amplitudes and those calculated for the structure. C involves the close, nonbonded interatomic distances, d_i, which are driven beyond normally accepted contact limits. The quantities e_k, ω_m, and k_i are weights. The term L involves constraints, G_n, which become zero when residue connectivity has been achieved and the λ_n are Lagrange multipliers. Competing molecular structures were assessed for significant differences by use of Ω, X, or C in Hamilton's test[31].

RESULTS

X-ray diffraction patterns. — A typical diffraction pattern obtained from potassium kappa-carrageenan (Fig. 1a) may be compared with a pattern from an oriented polycrystalline fiber of calcium iota-carrageenan[9] (Fig. 1b). The kappa-carrageenan pattern consists of continuous diffracted intensity distributed along layer lines, showing that the molecules are oriented with their long axes approximately parallel but that there is no lateral organization[32]. The continuous intensity is proportional to the cylindrical average of the squared amplitude of the Fourier transform a single molecule[32–34]. The layer-line spacings correspond to a molecular repeat distance of 25.0 Å.

Meridional diffracted intensity is present on the sixth and ninth layer lines, indicating that the molecule forms a three-fold helix. Another prominent feature of the diffraction pattern is the near absence of diffracted intensity on the first layer line for values of the reciprocal space cylindrical radius $R <\sim 0.15$ Å^{-1}. This is

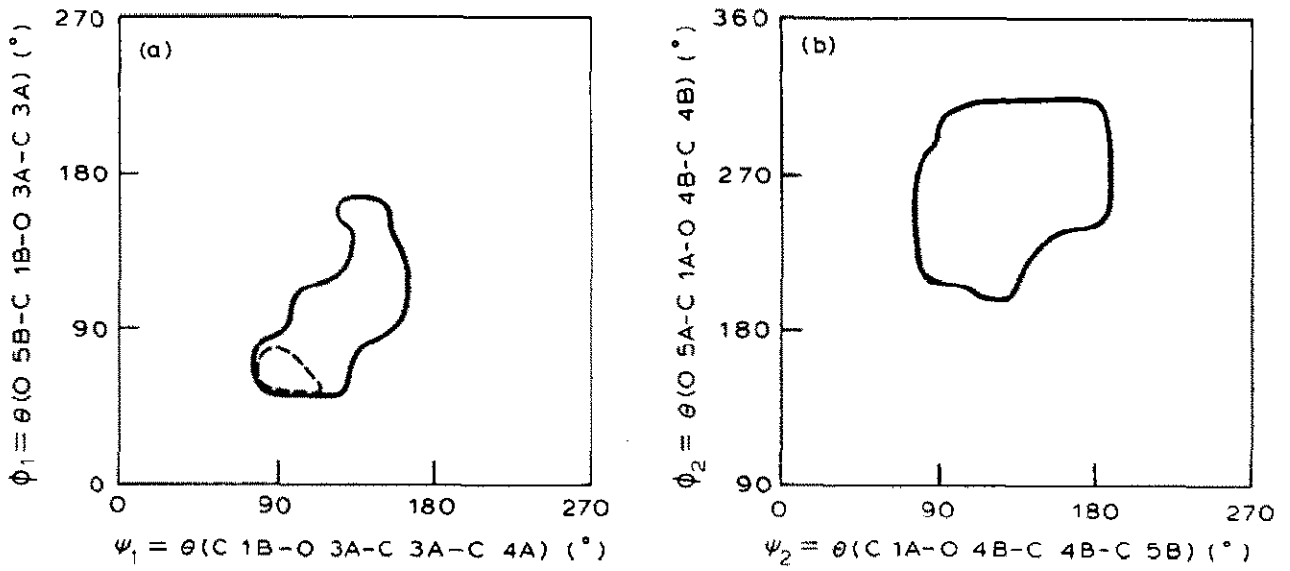

Fig. 2. Hard sphere maps for the (1→3)- (a) and (1→4)-linkages (b) in kappa-carrageenan with (----) and without (——) the sulfate at C-2 on the anhydrogalactose unit.

potentially very discriminating since such a distribution of diffracted intensity is difficult to achieve with certain classes of molecular model.

Molecular models. —To determine the range of conformation angles sterically allowed at the two glycosidic linkages, hard-sphere maps[9] were calculated for the two linkages (Fig. 2), both with and without a sulfate half-ester group at O-2 (in the staggered position). The sterically allowed regions are quite small and the "standard" (ϕ,ψ) values are at the centers of these regions. Note that removal of the sulfate group at O-2 (as in kappa-carrageenan) considerably widens the range of conformations available at the (1→3) linkage but has no influence on the (1→4) linkage.

Single chain molecular models of the polyanion with the required pitch and

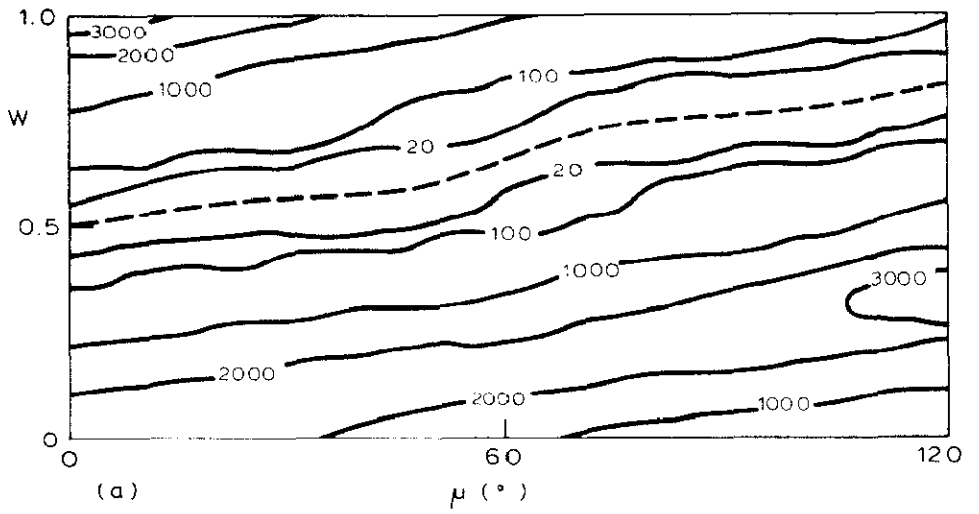

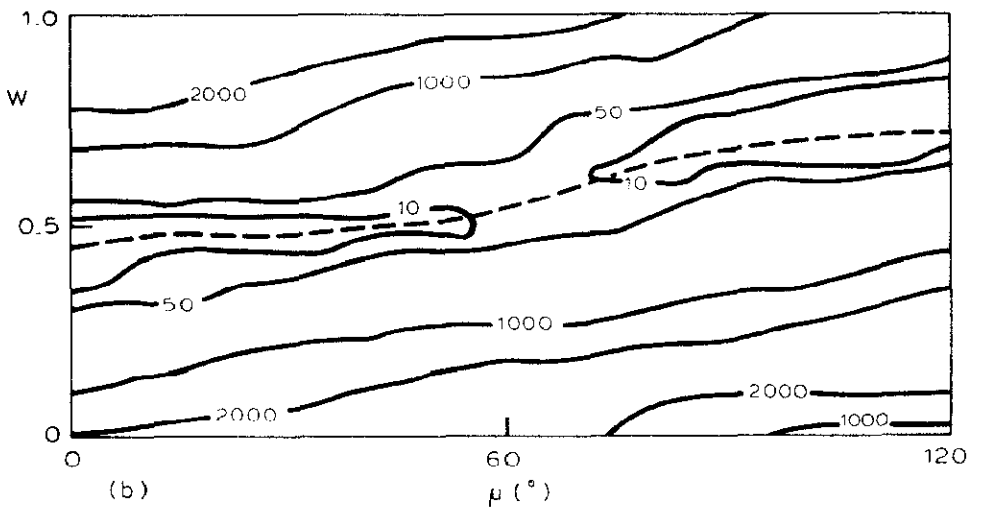

Fig. 3. Intermolecular steric compression (C), in arbitrary units, as a function of the relative orientation (μ) and translation (w) (as a fraction of the c-repeat) of the two chains for parallel (a) and antiparallel (b) right-handed double-helices. The broken lines indicate the centers of bands of low steric compression.

chirality were generated with the LALS technique. Both left- and right-handed models free of steric compression could be constructed. No intra-strand hydrogen bonds were evident in these models, as for iota-carrageenan[9].

Possible juxtapositions of single chains to form coaxial double helices were explored by calculating maps of the steric compression [the term C in Eq. (1)] as a function of the relative orientation (μ) and axial displacement (w) of the two chains. The steric compression for both parallel and anti-parallel double helices containing left-handed chains was very high for all values of μ and w. Short contacts could not be relieved even when μ and w were corefined with the bridge and side-chain conformations, so double helices with left-handed chains were discarded as possible molecular models. The steric compressions for the double helices with right-handed, parallel and antiparallel chains were low along bands in (μ,w) space in each case (Fig. 3) so that a wide variety of right-handed double helices are sterically possible.

The observed layer-line spacings and meridional reflections are also compatible with half-staggered double helices containing six-fold chains of pitch 50.0 Å. Molecular models of this type containing left- and right-handed chains could be generated free of steric compression.

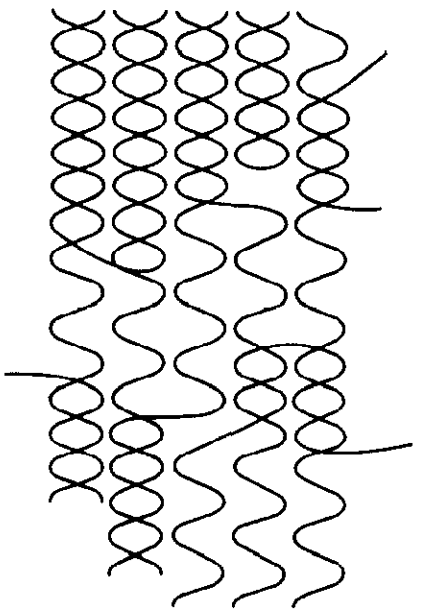

Fig. 4. Morphological model of a kappa-carrageenan fiber containing single helical links between iota-like double helices resulting in a statistical mixture of single and double helices.

The failure of kappa-carrageenan molecules to form strongly periodic lateral packings might simply be because the molecules are very "sticky" and can aggregate in a variety of different ways. On the other hand, there is no obvious chemical reason for kappa-carrageenan not to form half-staggered double helices similar to iota-carrageenan. We, therefore, considered a model containing a mixture of single and half-staggered (iota-like) double helices. Such a model would represent a specimen in which half-staggered double helices are linked by single-helical segments (Fig. 4). The crosslinks are assumed to be randomly distributed and the single- and double-helix sections longer than the coherence length of the molecules so that the coherent (layer line) diffracted intensity on the lth layer line $I_l(R)$ is given by Eq. (*2*)

$$I_l(R) = \alpha I_l^s(R) + (1 - \alpha) I_l^d(R) \qquad (2)$$

where the superscripts s and d indicate the intensity diffracted by single and double helices, respectively, and α is the (mean square) proportion of the ordered part of the specimen containing single helices. The double-helix term in Eq. (*2*) does not contribute to the odd layer lines so that $I_l(R) = \alpha I_l^s(R)$ (Eq. *3*), l being odd.

Refinement and comparison of alternative models. — Double helices with parallel chains vs. *single helices.* The layer-line spacing showed that kappa-carrageenan does not form half-staggered parallel double helices similar to those of iota-carrageenan. The first question, therefore, is whether the diffraction data can distinguish between single helices and minor variations on an iota-like structure. Left- and right-handed single-helix models and double-helix models containing parallel right-handed chains were therefore refined against the continuous X-ray data. To ensure that all possible juxtapositions of the two chains in the double-helix models would be trapped, refinements were started at values on a grid in (μ,w)

TABLE I

STATISTICS OF REFINED MOLECULAR MODELS OF KAPPA-CARRAGEENAN

Model	*Left or right*	*Single or double*	*Parallel or anti-parallel*	μ^a	w^b	X	N_x	C	N_c	Ω	N	$\hat{\Omega}^c$	*R*	*R''*
1	L	S				193	151	42	42	243	204	1.32	0.33	0.39
2	R	S				191	151	45	39	242	201	1.32	0.32	0.41
3[d]	R	D	P	28	0.54	90	151	47	45	144	209	1.00	0.23	0.27
4	R	D	P	25	0.61	97	151	50	45	152	209	1.03	0.23	0.28
5	R	D	A	27	0.46	125	151	52	43	184	207	1.14	0.26	0.31
6	R	D	A	47	0.61	142	151	52	46	200	210	1.18	0.29	0.34
7	R	D	A	80	0.63	144	151	47	41	197	205	1.18	0.29	0.34
8	R	D	A	102	0.65	123	151	56	47	185	211	1.13	0.25	0.31
9	R	D	A	88	0.69	133	151	47	40	185	204	1.15	0.28	0.32
10	R	D	A	103	0.79	113	151	46	41	165	205	1.08	0.26	0.30
11	R	D	A	117	0.83	107	151	61	48	174	212	1.09	0.24	0.29

[a](μ) Rotation of second chain relative to first (°). [b](w) Shift of second chain relative to first chain along the molecular axis as a fraction of the c-repeat. [c]($\hat{\Omega}$) Ratio of $(\Omega/N)^{1/2}$ to that for model **3**. [d]Best model.

space in the regions of low steric compression (Fig. 3). The grid spacings were $\Delta\mu = 20°$ and $\Delta w = 0.05$, and the range of values $0° < \mu < 60°$ and $0 < w < 1$ covers all nonsymmetry-related juxtapositions of the two chains. All the models free of over-short contacts resulting from these refinements are listed in Table I (models **1–4**). R and R'' are the conventional and quadratic X-ray R-factors respectively.

Both the left- and right-handed single-helix models are inferior to all the parallel double-helix models owing to their poor X-ray agreements. This is particularly pronounced on the first layer where the single helix models predict a strong peak in the region of $R = 0.06$ Å^{-1} in contradiction to the observations (Fig. 5). Since the sulfate groups contribute substantially to the X-ray scattering, for the single helices we explored the two alternative staggered conformations for θ (C 3A–C 4A–O 4A–SA), but these produced many unacceptable short contacts. Refinements were also conducted for single helices in which the sulfate group conformation was randomly distributed in the allowed domain with half-widths of the deviation up to 30°. In no case did this improve the X-ray agreement. We also examined a parallel double-helix model in which the two chain backbones have identical conformations and are half-staggered (as in iota-carrageenan) but the sulfate and hydroxymethyl groups are allowed different conformations in the two chains. However, in the resulting model, there was little difference in the sulfate group conformations leading to weak calculated diffraction on the odd layer lines and, hence, poor agreement with the X-ray data ($R = 0.5$).

On the basis of both the total discrepancy Ω and the X-ray discrepancy X, the single-helix models could be rejected over all the parallel double-helix models at the 99.5% confidence level. The best parallel double-helix model (**3**) is offset only slightly by a rotation of 28° and a translation of 1.0 Å from the half-staggered

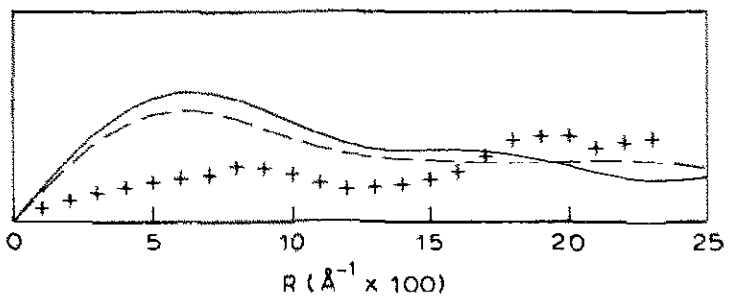

Fig. 5. Calculated amplitudes of cylindrically averaged Fourier transforms on the first layer line of the refined right (——) and left handed (----) single helix models compared with the measured values (+). For the calculated amplitudes, the scattering factors are water weighted[35], and an isotropic temperature factor B = 6.0 Å^2 has been applied.

position. Another model (**4**), almost as good, contains parallel chains with a similar rotation (25°) but translated further (2.8 Å) from the half-staggered position. There was no significant difference between these two models on the basis of the X-ray agreement or the total discrepancy Ω. The important finding was that double-helical models that are related to the iota structure are convincingly superior to single helices as possible molecular structures.

Model **3** was chosen as a representative double-helix structure for kappa-carrageenan. Since the two chains are in different environments, their conformation will in general be different. The symmetry of the model was, therefore, relaxed by not requiring the two strands to be conformationally identical. Although the conformations of the two chains changed, the average difference between the glycosidic conformation angles and those of the model with identical chains was small ($\langle\Delta\theta\rangle$ = 8°), and there was no improvement in the X-ray agreement. We, therefore, concluded that any conformational differences between the two chains are too small to be supported by the data available in this analysis. The representative model **3**, therefore, has identical chains. The conformation angles and calculated molecular transform are shown in Table II and Fig. 6, respectively. Meridional reflections are difficult to measure accurately but comparison of Fig. 1a

TABLE II

CONFORMATION ANGLES AND CHAIN JUXTAPOSITIONS OF THE BEST PARALLEL DOUBLE-HELIX STRUCTURE (MODEL **3**) OF KAPPA-CARRAGEENAN COMPARED WITH THOSE OF IOTA-CARRAGEENAN

Conformation angle	*Type*	*Value (degrees)*		
		Kappa	*Standard*	*Iota*
θ(O 5B–C 1B–O 3A–C 3A)	(1→3)-linkage ϕ_1	61	90	77
θ(C 1B–O 3A–C 3A–C 4A)	ψ_1	81	120	79
θ(O 5A–C 1A–O 4B–C 4B)	(1→4)-linkage ϕ_2	−97	−100	−87
θ(C 1A–O 4B–C 4B–C 5B)	ψ_2	108	130	81
θ(C 3A–C 4A–O 4A–SA)	*Sulfate group*	−121	−120	−125
θ(C 4A–O 4A–SA–OS 1A)		−155	180	−159
θ(C 4A–C 5A–C 6A–O 6A)	*Hydroxymethyl group*	−179	145	175
μ		28		0
w		0.54		0.50

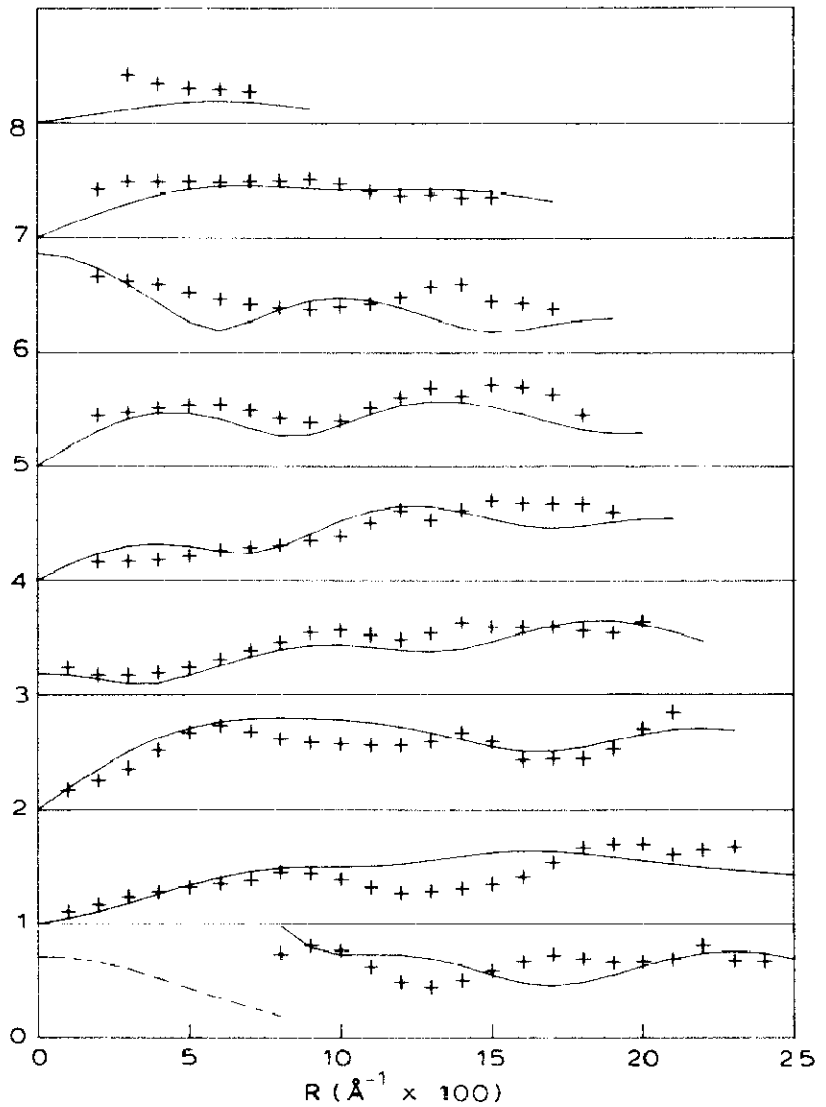

Fig. 6. Calculated amplitude (——) of the cylindrically averaged Fourier transform of the best (parallel) double helix structure (model **3**) of kappa-carrageenan compared with the measured values (+). The broken curve represents the calculated amplitude divided by 5. Amplitudes are calculated as described in the caption to Fig. 5.

and Fig. 6 showed good qualitative agreement—weak and strong on the third- and sixth-layer lines, respectively. Mutually perpendicular views of the structure are shown in Fig. 7 and compared to iota-carrageenan. One of the two O-6A–O-2A interchain hydrogen bonds per disaccharide in iota-carrageenan is retained in the kappa-carrageenan structure (Fig. 7).

Double helices with antiparallel chains. Double-helix models containing antiparallel chains were refined starting from a variety of positions in (μ,w) space in the region of low steric compression in the range $0° < \mu < 120°$ and $0 < w < 1$. The models free of over-short contacts obtained are listed in Table I (models **5–11**). Each of these models is inferior to the parallel models **3** and **4** at the 99.5% confidence level on the basis of Ω. However, some of them are not significantly inferior to the parallel models on the basis of the X-ray agreement alone. Although the models with parallel chains are preferred, there is a remote possibility that better X-ray data would favor models with antiparallel chains.

Other models. Half-staggered double-helical models containing six-fold chains produced poor fits with the X-ray data for both the left-handed ($R = 0.43$, $R'' = 0.50$) and right-handed ($R = 0.40$, $R'' = 0.48$) cases, and were discarded.

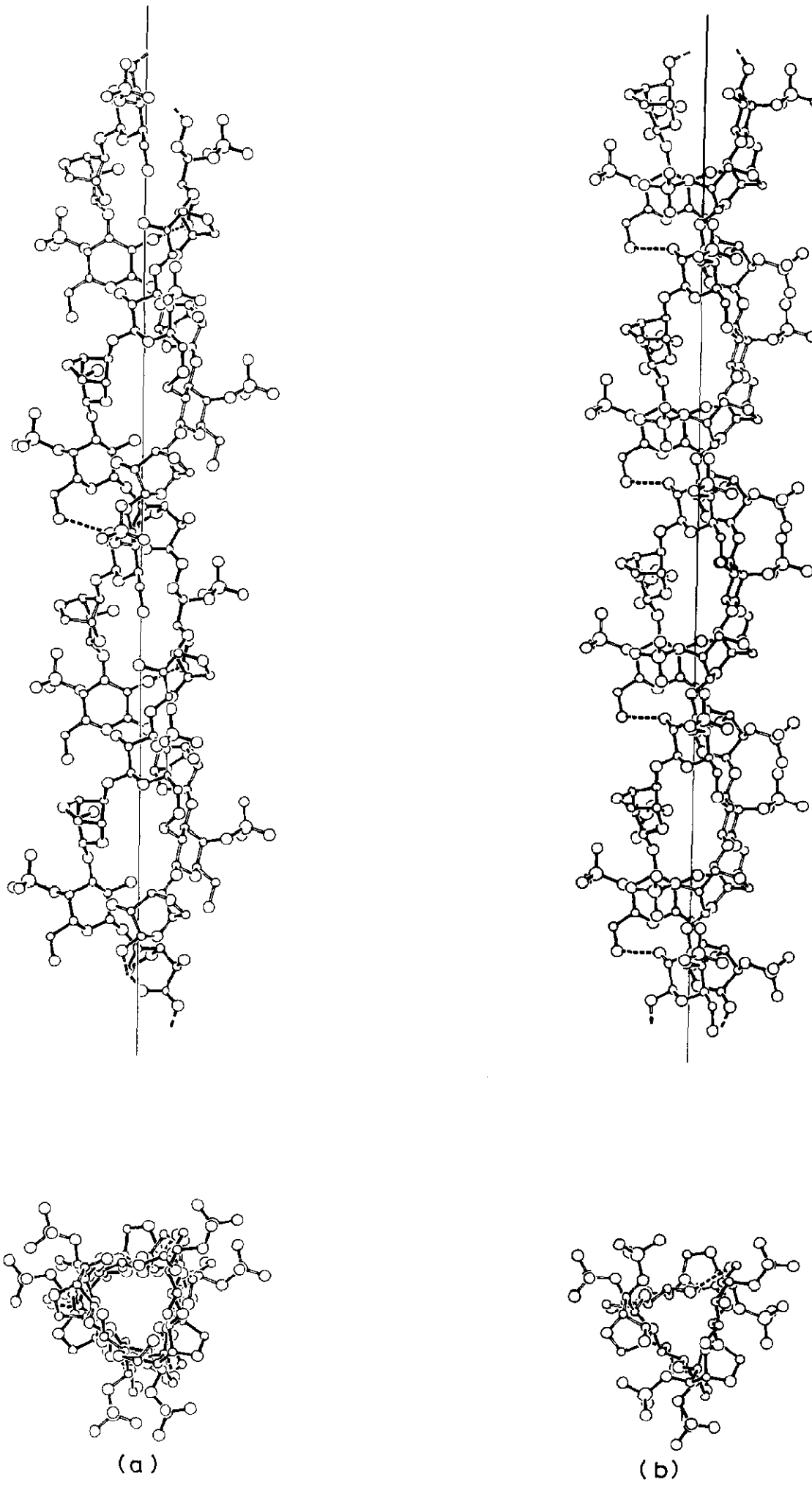

Fig. 7. Mutually perpendicular views of (a) the best refined (parallel) double-helix structure (model **3**) for kappa-carrageenan compared with (b) iota-carrageenan. The two chains are shown with open and full bonds, and the O-6A–O-2A hydrogen bonds by broken lines. The projection of kappa-carrageenan along the molecular axis appears more cluttered than iota-carrageenan since, in the later case (because of the half-staggering) half of the atoms are eclipsed.

For a model containing a mixture of single helices and iota-like duplexes (Fig. 4), inspection of Eq. (*3*) showed an immediate difficulty because of the discrepancy (noted above) between the transform of the single-helix models and that observed on the first layer line. A refinement of the right-handed single-helix model against the X-ray data on only the odd-layer lines gave discrepancies of $R = 0.47$ and $R'' = 0.50$ (on the odd-layer lines only). Since the presence of half-staggered double-helical segments would suppress the resultant amplitude on the first (and in fact all the odd) layer lines, the transform intensities of the right-handed single-helix model and a sterically refined half-staggered right-handed, parallel, double-helix model were used in the right side of Eq. (*2*), and refined against the observed X-ray data on all layer lines by varying α and an X-ray scale factor. The best X-ray agreement was at $\alpha = 0.80$ giving $R = 0.32$ and $R'' = 0.39$, which is litlle different from that of the right-handed single helix alone. We concluded, therefore, that a model of this type is not consistent with the diffraction data.

We examined also the compatibility of the X-ray data with kappa-carrageenan dimers in which the two strands are not coaxial but associate in a side-by-sidc fashion. The individual strands of the dimer would probably be threefold helices of the type defined. The number of possible models of this type is very large and we did not consider it fruitful to confront them all with the limited diffraction data available. However, one general aspect of the diffraction data indicated that side-by-side dimers are unlikely. The maximum radius of such molecules would be approximately twice the radius of a single strand. The consequences of this difference in radius for the diffraction pattern were assessed as follows. At low resolution, the cylindrically averaged electron density of any structure projected along the molecular axis can be crudely approximated by a cylinder of constant electron density and radius equal to the maximum radius of the molecule. The amplitude of the scattering at low resolution by such a cylinder can be compared to the observed amplitude on the equator. The amplitude $A(R)$ of the Fourier transform of a circular cylinder of radius a is $A(R) = |J_1(2\pi Ra)|/R$ (Eq. *4*) where J_1 is the first-order Bessel function of the first kind. The maximum radius of both the single and coaxial double helix structures defined above is approximately 7.5–10.0 Å depending on how well organized the water layer on the molecular surface might be. Allowing for 2 Å of interpenetration, the radius of a (cylindrically averaged) side-by-side dimer would be ~14.0–16.5 Å. $A(R)$ for cylinder radii of 9.0 Å and 15.0 Å are shown in Fig. 8 together with the amplitude measured on the equator. The first maximum of $A(R)$ for a cylinder radius of 9 Å corresponds closely to the first peak in the observed amplitude at $R = 0.09$ Å^{-1}. For a cylinder radius of 15.0 Å, the first peak of $A(R)$ is at a much smaller value of R. The diffraction data, therefore, favor a coaxial dimer over a side-by-side dimer.

DISCUSSION

Our results indicated that kappa-carrageenan forms double rather than single

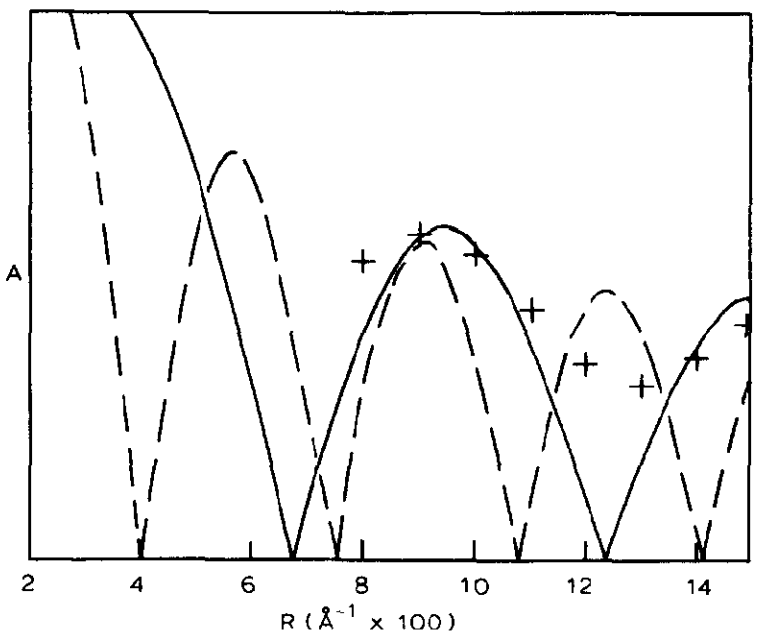

Fig. 8. Calculated amplitudes of the Fourier transforms (on arbitrary scales) of homogeneous circular cylinders of radius 9.0 Å (——) and 15.0 Å (----) compared with the amplitude observed (+) on the equator of the kappa-carrageenan diffraction pattern. The calculated amplitude has been multiplied by R to enhance it at high resolution.

helices in the condensed state. Double helices with parallel chains, similar to those formed by iota-carrageenan, but with the chains offset from the half-staggered position by ~28° about and 1.0 Å along the helix axis predict diffracted intensities in good agreement with those observed. This relatively small morphological change from the structure of iota-carrageenan is the minimum that produces sufficient diffracted intensity on the odd layer lines. A number of double-helical models with antiparallel chains could be generated that are free of steric compression and also predict diffraction amplitudes in reasonable agreement with those observed. These models are inferior to the best parallel chain models in terms of both X-ray agreement and overall discrepancy, but we did not consider the differences significant enough utterly to exclude an antiparallel chain duplex. Duplexes containing six-fold chains, structures containing a mixture of single and iota-like double helices, and non-coaxial dimers are certainly inconsistent with the diffraction data.

The best (parallel) double-helical structure has conformations at the (1→3) linkage similar to those of iota-carrageenan (average difference between the kappa and iota structures is $\langle\Delta\theta\rangle = 9°$), despite the greater conformational freedom allowed by the absence of the sulfate group at O-2B. There is, however, a larger difference in the (1→4) linkage conformations between the kappa- and iota-carrageenans ($\langle\Delta\theta\rangle = 18°$) that cannot be due to the absence of the sulfate group at O-2B (Fig. 2). It could be due to the different juxtapositions of the two chains in kappa- and iota-carrageenan or to the difference in pitch ($\Delta P = 1.6$ Å) between the two structures, which produces a compression along the molecular axis of 0.5 Å per disaccharide unit in kappa-carrageenan. The conformation of the sulfate group differs little from that in iota-carrageenan ($\langle\Delta\theta\rangle = 4°$).

Although the absence of the anhydrogalactose sulfate group increases the flexibility of the kappa-carrageenan chain over that of iota-carrageenan, it is not

clear why kappa-carrageenan does not adopt a half-staggered conformation similar to that of iota-carrageenan. Indeed, a stereochemically acceptable half-staggered, parallel double-helix model with a pitch of 25.0 Å could be constructed for kappa-carrageenan that incorporates only slightly stretched (by < 0.1 Å) O-6$\cdots$O-2 hydrogen bonds that occur in iota-carrageenan. Our representative double-helix structure for kappa-carrageenan has only one intermolecular hydrogen bond per disaccharide units in contrast to iota-carrageenan which has two. The additional steric restrictions imposed on iota-carrageenan by the anhydrogalactose sulfate group, as well as the loss of a free hydroxyl group, may force it to adopt a configuration different to that of kappa-carrageenan. To explore the consequences of small departures of iota-carrageenan from the half-staggered conformation, steric refinements were conducted with the two chains forced to be slightly offset from the half-staggered position. Axial shifts of 0.5 Å stretched one of the O-6A$\cdots$O-2A hydrogen bonds to 3.1 Å, and axial shifts of 1.0 Å disrupted both hydrogen bonds and introduced over-short interatomic contacts. The structure reverted to the half-staggered position when freely refined. Hence, the small departures from half-staggering available to kappa-carrageenan appear to be unfavorable for iota-carrageenan.

ACKNOWLEDGMENTS

The authors thank the National Science Foundation for support (grants 8512599 and 8606942) and Robert Werberig for photography.

REFERENCES

1 M. GLICKSMAN, in M. GLICKSMAN (Ed.), *Food Hydrocolloids*, CRC Press, Boca Raton, 1983, Vol. 2, pp. 73–113.
2 G. A. TOWLE, in R. L. WHISTLER AND J. N. BEMILLER (Eds.), *Industrial Gums*, 2nd ed., Academic Press, New York, 1973, pp. 83–114.
3 W. YAPHE, *Can. J. Bot.*, 37 (1959) 751–757.
4 D. A. REES, *Adv. Carbohydr. Chem. Biochem.*, 24 (1969) 267–332.
5 E. R. MORRIS, D. A. REES, AND G. ROBINSON, *J. Mol. Biol.*, 138 (1980) 349–362.
6 M. DUCKWORTH, K. C. HONG, AND W. YAPHE, *Carbohydr. Res.*, 18 (1971) 1–9.
7 I. C. M. DEA AND D. A. REES, *Carbohydr. Polym.*, 7 (1987) 183–224.
8 N. S. ANDERSON, J. W. CAMPBELL, M. M. HARDING, D. A. REES, AND J. W. B. SAMUEL, *J. Mol. Biol.*, 45 (1969) 85–99.
9 S. ARNOTT, W. E. SCOTT, D. A. REES, AND G. C. A. MCNAB, *J. Mol. Biol.*, 90 (1974) 253–267.
10 D. A. REES, *J. Chem. Soc.*, (1963) 1821–1832.
11 D. A. REES, W. E. SCOTT, AND F. B. WILLIAMSON, *Nature (London)*, 227 (1970) 390–392.
12 D. S. REID, T. A. BRYCE, A. H. CLARK, AND D. A. REES, *Faraday Discuss. Chem. Soc.*, 57 (1974) 230–237.
13 R. A. JONES, E. J. STAPLES, AND A. PENMAN, *J. Chem. Soc., Perkin Trans. 2*, (1973) 1608–1612.
14 I. C. M. DEA, A. A. MCKINNON, AND D. A. REES, *J. Mol. Biol.*, 68 (1972) 153–172.
15 C. ROCHAS AND M. RINAUDO, *Biopolymers*, 19 (1980) 2165–2175.
16 I. T. NORTON, D. M. GOODALL, E. R. MORRIS, AND D. A. REES, *J. Chem. Soc., Chem. Commun.*, (1979) 988–990.
17 C. ROCHAS AND M. RINAUDO, *Biopolymers*, 19 (1980) 1675–1687.
18 C. ROCHAS AND J. MAZET, *Biopolymers*, 23 (1984) 2825–2833.

19 S. PAOLETTI, O. SMIDSRØD, AND H. GRASDALEN, *Biopolymers,* 23 (1984) 1771–1794.
20 O. SMIDSRØD, I. ANDRESEN, H. GRASDALEN, B. LARSEN, AND T. PAINTER, *Carbohydr. Res.,* 80 (1980) c11–c16.
21 H. GRASDALEN AND D. SMIDSRØD, *Macromolecules,* 14 (1981) 1842–1845.
22 R. P. MILLANE AND S. ARNOTT, *J. Appl. Crystallogr.,* 18 (1985) 419–423.
23 R. P. MILLANE AND S. ARNOTT, *J. Macromol. Sci. Phys.,* B24 (1985) 193–227.
24 W. FULLER, F. HUTCHISON, M. SPENCER, AND M. H. F. WILKINS, *J. Mol. Biol.,* 27 (1967) 507–524.
25 R. D. B. FRASER, T. P. MACRAE, A. MILLER, AND R. J. ROWLANDS, *J. Appl. Crystallogr.,* 9 (1976) 81–94.
26 L. MAKOWSKI, *J. Appl. Crystallogr.,* 11 (1978) 273–283.
27 S. ARNOTT AND W. E. SCOTT, *J. Chem. Soc., Perkin Trans. 2,* (1972) 324–335.
28 J. W. CAMPBELL AND M. M. HARDING, *J. Chem. Soc., Perkin Trans. 2,* (1972) 1721–1723.
29 S. ARNOTT AND A. J. WONACOTT, *Polymer,* 7 (1966) 157–166.
30 P. J. C. SMITH AND S. ARNOTT, *Acta Crystallogr., Sect. A,* 34 (1978) 3–11.
31 W. C. HAMILTON, *Acta Crystallogr.,* 18 (1965) 502–510.
32 S. ARNOTT, *ACS Symp. Ser.,* 141 (1980) 1–30.
33 R. D. B. FRASER, T. P. MACRAE, D. A. D. PARRY, AND E. SUZUKI, *Polymer,* 12 (1971) 35–56.
34 S. ARNOTT, R. CHANDRASEKARAN, R. P. MILLANE, AND H. S. PARK, *J. Mol. Biol.,* 188 (1986) 631–640.
35 R. D. B. FRASER, T. P. MACRAE, AND E. SUZUKI, *J. Appl. Crystallogr.,* 11 (1978) 693–694.